Research article

Radon concentration and affecting environmental conditions in water-curtain heated cultivation facilities

Yelim Nam [a], Sangin Kim [a], Jihong Shin [a], Chaewon Yi [a], Kyoung Sook Jeong [b], Seung Kyu Lee [c], Jiyoung Ko [d], Jongjin Lee [d,*]

[a] ARIM SCIENCE Inc., 918, 66, Daehwa-ro 106 Beon-gil, Daedeok-gu, Daejeon, 34365, Republic of Korea
[b] Department of Occupational and Environmental Medicine, Wonju Severance Christian Hospital, Wonju College of Medicine, Yonsei University, 20, Ilsan-ro, Wonju, Gangwon-do, 26426, Republic of Korea
[c] Korea Atomic Energy Research Institute, 989-111, Daedeok-daero, Yuseong-gu, Daejeon, 34057, Republic of Korea
[d] Department of Physics and Research Institute of Natural Science, Gyeongsang National University, Jinju, 52828, Republic of Korea

ARTICLE INFO

ABSTRACT

Farmers cultivate plants in the winter using water curtain cultivation (WCC) facilities by spraying groundwater to keep them warm. In this study, the WCC facilities exhibited high radon concentrations during winter. The risk varied significantly depending on the facility operation, peaking in the early morning and then decreasing upon ventilation. At all measurement sites, radon concentrations were low when groundwater was not used. Even during the period of facility groundwater use, if water vapor condensation does not occur, there is no significant difference from soil-only emissions. However, once water vapor condensation occurs, radon accumulates rapidly, depending on the degree of radon contamination in the groundwater. Because groundwater contamination varies according to dilution by regional rainfall or inflow from other regions due to groundwater movement, abnormal changes in radon content occur. We found that in the absence of water vapor condensation in the facility, all the radon emitted from the soil and groundwater quickly escaped to the atmosphere, resulting in significantly lower indoor radon concentrations. These findings pave the way for the development of new methods to mitigate radon in WCC facilities.

1. Introduction

Radon is a colorless, odorless, inert gas and the daughter nuclide of thorium and uranium. ^{220}Rn has a short half-life of 55 s, whereas ^{222}Rn, a daughter nuclide of uranium, has a half-life of 3.8 days; thus, ^{222}Rn is primarily responsible for environmental impacts. When inhaled as a gas, radon leads to lung cancer by causing alpha decay, leaving radon progeny in the alveoli [1]. Unlike other inert gases, radon is soluble in water and is present at high concentrations in groundwater, where it can cause stomach cancer when consumed [2]. It accounts for 3–14 % of all lung cancers worldwide [3]. The US Environmental Protection Agency classifies radon as a lung carcinogen in nonsmokers, and radon is responsible for 21,000 deaths annually in the United States [4]. To recognize

---

the radon risk, the Korean government introduced indoor radon management standards through the Indoor Air Quality Management Act in December 2016. An indoor recommended standard for determining radon concentration (148 Bq/m^3) has been established [5].

Radon is present at high concentrations in granitic soils. When the water table passes through it, it enters the water, migrates, and is released into the atmosphere [6]. High radon concentrations have been found in the basements of buildings in contact with the ground and can diffuse into living spaces [7].

Agricultural greenhouses carry a greater risk of radon exposure than typical buildings because of the abundance of exposed soil, and farmers working in the early morning are exposed to radon that accumulates nightly in sealed greenhouses [8,9]. Water curtain cultivation (WCC) facilities spray groundwater to form a water film on the inner houses for heat insulation in the winter season, which leads to an additional risk of radon in the groundwater being released into the air [10,11]. A case study showed that radon concentrations in three nearby WCC facilities reached a few thousand Bq/m^3 and varied greatly among the measuring sites [12]. The maximum values occurred at dawn and then decreased with increasing ventilation, similar to those in an ordinary greenhouse. However, the origin and detailed dynamics of radon accumulation have not been specified because of a lack of other information [12].

Unlike in inhabited houses and ordinary greenhouses, studies on radon concentrations in WCCs are scarce, particularly regarding their origin and accumulation dynamics. This study aimed to determine the dynamics of radon accumulation in WCCs by continuously monitoring related environmental variables such as temperature, pressure, and relative humidity as the inert gas of radon moves along the gradient of these variables. By investigating these variables throughout the growing season and at multiple sites, we found that heavy radon concentrations originated from contaminated groundwater. The accumulation dynamics were mainly determined by the structural ventilation and water vapor condensation on the polymer film surface. These findings provide new insights for mitigating high radon concentrations in WCC facilities.

2. Materials and methods

2.1. Location and measurement sites

Fifteen WCC facilities in Sancheong-gun, Gyeongsangnam-do, were selected for data collection. The geographical, topographical, and positional features of the installation locations are shown in Fig. 1. The study area is east of Mount Jiri, and its geology mainly consists of Paleoproterozoic metasedimentary migmatitic and granitic gneisses [13]. This county and its nearby areas are famous for cultivating strawberry plants in the winter using WCC facilities. Fifteen sites (A1 to A15) were selected based on the distribution of the administrative districts. In this study, only the most commonly adopted building structure, metal-frame double polyethylene (PE) film
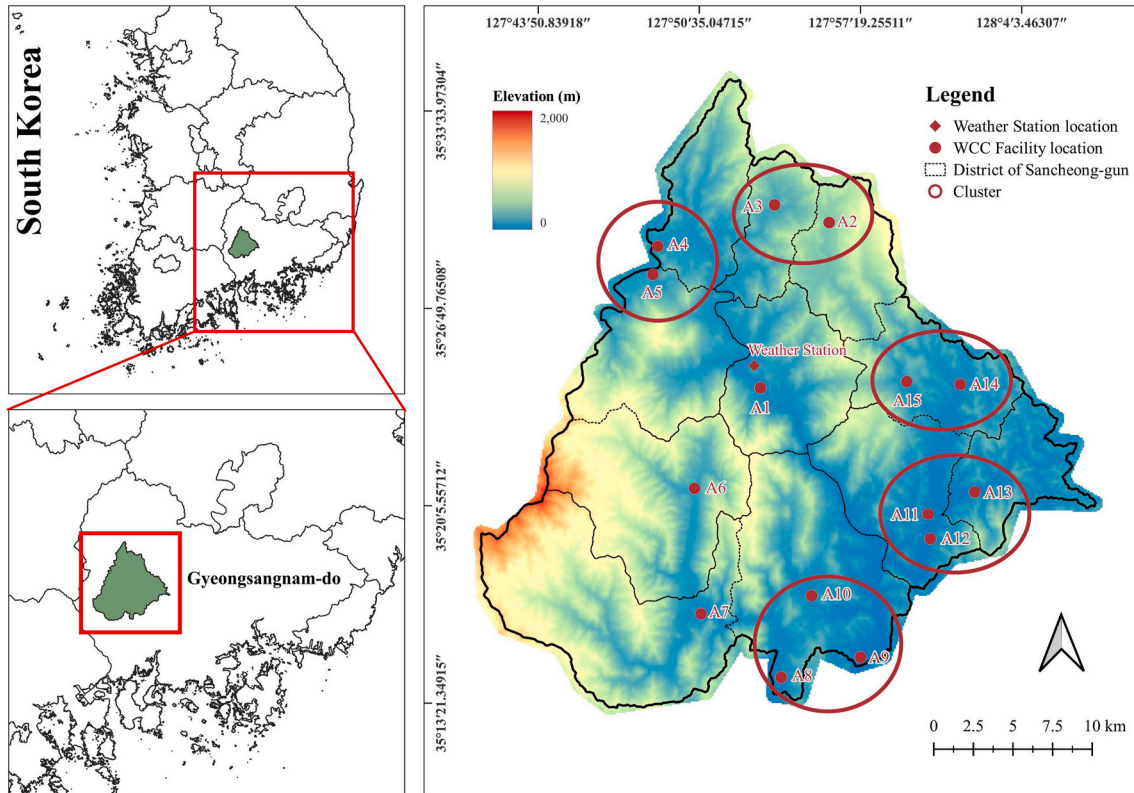

Fig. 1. Regional and local map of Sancheong County. All 15 measurement sites and a weather station.

encapsulation, was chosen to avoid structural dependency.

2.2. Radon gas concentration measurements

In this study, an IoT-based real-time air quality monitoring system was used. We measured the radon concentration and other environmental factors during the entire period of WCC cultivation for 141 days from December 11, 2022, to April 30, 2023. Our measurement unit (Model ArimAir OA200W, Arim Science Inc.) can simultaneously measure particulate matter (<2.5 μm), radon, air pressure, temperature, and relative humidity, transmitting measurement data to a data center (server) via a 4G wireless communication network. The unit has acquired class one certification as portable equipment with 90.8 % accuracy, according to the Korean Ministry of Environment; detailed specifications are listed in Table 1. The air fan created an airflow from the bottom air inlet to the top of the unit. The air is then redirected to the bottom air outlet, where it diffuses into the pulse ionization chamber (PIC), and the degree of alpha particle decay is counted [14]. A schematic diagram of this unit is shown in Fig. 2(a). The radon concentration data were calculated as the 10-min average of the decay events. One-hour averages of the values were used to smooth out the statistical scatter [15]. The OriginPro 8 software (OriginLab) was used to analyze the data. The advantage of the PIC is that it is insensitive to relative humidity, and it was reported that less than 5 % accuracy error was achieved under 65 % relative humidity [16]. However, if water vapor condenses at 70 % or above, condensed water drops tend to capture electric charges and reduce collection efficiency [17]. Thus, the actual radon concentration >70 % humidity was greater than the measured value.

2.3. Continuous monitoring of humidity, temperature, and air pressure

A measuring device was installed inside the facility 1.2–1.5 m above the ground, as shown in Fig. 2(b), following the Indoor Air Sampling And Evaluation Method (ES 02130. d) [18]. Simultaneously, air pressure, temperature, and humidity data were measured and updated at 1-min intervals, while radon was collected every 10 min. Aligning all variables to 1-h averages facilitated synchronization with important smoothed radon concentration values. In addition, this hourly averaging strategy enhances the ease of analysis of an extensive dataset. The number of data points collected during this period is listed in Supplementary Table 1. Facilities A1, A7, A10, A11, and A13 collected less data than other units because of frequent communication errors. This study used the regional temperature and raindrop data from the National Climate Data Center of the Korea Meteorological Administration to represent climatic conditions when needed [19].

2.4. Regional correlation analysis

To analyze the radon profiles at the sites, the relative standard deviation (RSD) was used to determine the correlation between any two sites, i and j (Equation (1)).

The day's representative value was first obtained by averaging all the measured values over a day. The daily similarity was obtained by calculating the standard deviation ($SD_{day}(i,j)$) divided by the average radon concentration ($C_{day}(i,j)$) at the two sites (Equation (2)) [20,21]. The average over the entire measurement day was used as the RSD (i,j) value as shown below:

$$RSD(i,j) = \frac{1}{D} \sum_{day=1}^{D} SD_{day}(i,j) \Big/ C_{day}(i,j) \qquad (1)$$

$$SD_{day}(i,j) = \sqrt{\frac{\left(C_{i,day} - C_{day}\right)^2 + \left(C_{j,day} - C_{day}\right)^2}{2}}$$
$$C_{day}(i,j) = \frac{C_{i,day} + C_{j,day}}{2} \qquad (2)$$

In Equation (2), $c_{i,day}$ and $c_{j,day}$ represent the average concentrations of a particular day at sites i and j, respectively. The RSD was considered small if the two points showed similar values on all days. By contrast, the RSD was high when the values of the two points were statistically irrelevant.

Table 1
ArimAir OA200W specifications.

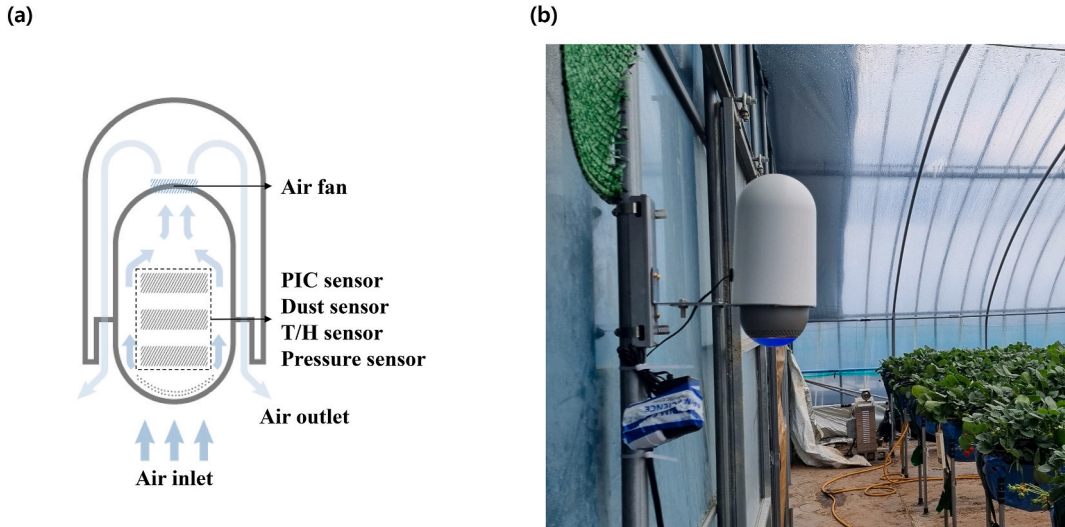| Specifications Description	Value
Radon sampling	Passive diffusion chamber
Detection method	Pulsed ionization chamber
Sensitivity	0.3 cpm/pCi/L
Minimum detectable concentration	7 Bq/m^3 (0.2 pCi/L)
Measurement range	7–3696 Bq/m^3 (0.2–99.9 pCi/L)
Dimension	Height: 243 mm, Ø: 115 mm
Certificated repeatability	92.3 %
Certificated accuracy	90.8 %

(a)

(b)

Fig. 2. Schematic and installation of the measurement unit: (a) cross-sectional schematic and airflow direction and (b) photograph of the installation setup (A2).

3. Results

Fig. 3 shows the time series plots of radon concentration, relative humidity, and air pressure with the recommended national standard guidelines at A12 and A15. A12 had a relatively low radon concentration, and the A15 had the maximum measured concentration of all 15 facilities. The minimum, maximum, and average radon concentrations at all study sites are listed in Table 2.

The pressure was the same at both locations, and there was day-to-day variation; however, the intraday pressure was not significantly different. However, humidity showed considerable variation, as in the case of the radon concentration. The indoor temperature
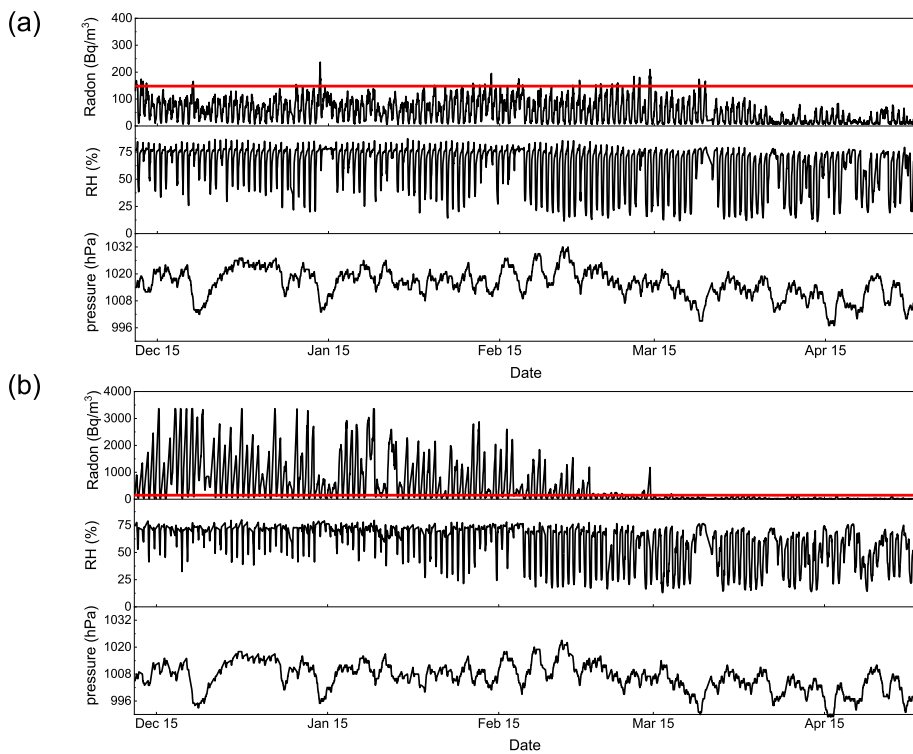

Fig. 3. Time series plots of radon concentration, RH, and air pressure at (a) A12, the lowest value site, and (b) A15, the highest value site. The recommended national standard has been added to the guide.

Table 2
Maximum, minimum, and average radon concentrations at all sites.

Site	Radon (Bq/m³)		
	MAX.	MIN.	AVG.
A1	370	3	79
A2	634	6	122
A3	643	6	137
A4	292	6	54
A5	224	5	47
A6	189	6	43
A7	214	6	41
A8	258	6	62
A9	2146	6	458
A10	682	6	182
A11	365	5	77
A12	250	6	57
A13	347	6	62
A14	989	5	147
A15	3363	6	480

increases during the day and stays constant at approximately 10 °C at night, depending on the WCC operation (not shown here). Therefore, humidity, among other factors, is closely related to daily radon concentration.

3.1. Radon trapping upon water vapor condensation

Fig. 4 shows the onset of radon accumulation at the water vapor saturation point at Site A3, whether groundwater was sprayed in February (a) or April (b). The scattered points of high radon and low humidity were collected during ventilation.

The humidity-radon graph in Fig. 4(a) shows that the radon concentration remained constant up to a relative humidity of 70 %, after which it increased rapidly. An increase in radon concentration near the water vapor saturation point has been observed in caves with limited atmospheric circulation [22]. Condensed water vapor significantly hampers radon diffusion, resulting in radon accumulation because the diffusion rate of radon in water is approximately 100 times lower than that in air. The concentration of radon increases slowly with increasing humidity as the water vapor saturation point approaches because of the time difference in gap filling according to the pore size distribution of the soil and rock. Subsequently, it increases rapidly at the saturation point [23].

In contrast, in the present study, the radon concentration changed slightly immediately before the saturation point. The concentration rapidly increases at the saturation point. This difference may originate from the fact that all the moisture molecules were at the same atmospheric pressure and temperature on a smooth surface [7].

When additional heat was applied, the temperature at the measurement height increased, resulting in a slight decrease in relative humidity. Thus, the relative humidity at high radon concentrations was between 60 and 80 %, whereas the starting point at which the radon concentration increased was 70 %. The saturation point was fixed without additional heating, as shown in Supplementary Fig. 1.

Notably, although the maximum radon concentration was relatively low in April, it increased near the water vapor saturation point, as shown in Fig. 4(b).
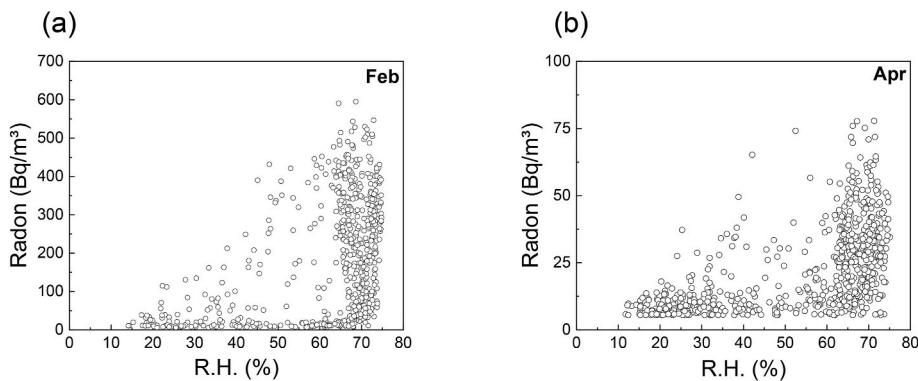

Fig. 4. Radon content accumulated significantly at the beginning of the water vapor saturation point in site A3 in (a) February, when groundwater was used, and (b) April, when groundwater was not used. Scattered points of high radon with low humidity values were collected during ventilation.

3.2. Correlations depending on regional distance

To compare the variational radon concentration characteristics based on the mutual distances between facilities, we calculated the distance between facilities (MDF) for all WCC facilities. Additionally, we formed clusters of adjacent facilities using the center coordinates of the members as the central coordinates of the cluster, as shown in Fig. 1. These centered coordinates enable the calculation of the mutual distances between clusters (MDC). Using the MDF and MDC methods, the pairs of facilities were classified into short, medium, and long groups.

Short group: pairs of facilities within the same cluster are considered candidates for a short group. Two pairs with the highest data acquisition rates were selected as representatives of the short group.

Medium group: Pairs with MDF values within ±10 % of the average MDC value (16.6 km) were considered candidates for the medium group. From these candidates, the two pairs with the highest data acquisition rates were selected as representatives of the medium group.

Long group: Pairs within two clusters with the highest MDC values were considered candidates for the long group. Two pairs with the highest data acquisition rates were selected as representatives of the long group.

Fig. 5 shows the day-averaged datasets for each distance group selected based on the data acquisition rate and shortest distance order. As the distance increased from short to long, the difference between the two day-averaged radon concentrations in each group became more significant. The RSD values are presented in Table 3. The obtained RSDs of the short-distance group were less than 0.2, but as the distance increased, the RSD values increased from 0.25 to 0.3 for the medium-distance group to as large as 0.5–0.6 for the long-distance group. Because lower RSD values imply that the radon concentration at the two sites behaved similarly, the average radon concentration and its variation were similar in the shorter-distance facilities. In contrast, long-distance facilities showed different levels and variational behaviors. The terrestrial homogeneity of neighboring sites can explain this regional homogeneity, which directly donates radon to the air [7] and groundwater [24].

3.3. Abnormal radon concentration fluctuation due to rain

As discussed in Section 3.2, the close regions exhibited similar radon concentration behaviors. However, there was a large difference in radon concentrations between A4 and A5 in mid-January, even with a high degree of adjacency. Fig. 6 shows a detailed view of the relative humidity and radon concentrations at sites A4 and A5 from January 10 to January 19. Radon concentrations decreased in A5 but increased in A4 following rain on January 13. A high RH value when opening a facility during the day indicates high humidity in the outside atmosphere; therefore, we can estimate the rainfall during this time. Using data from the National Climate Data Center, we found that 0.1 mm, 34.5 mm, 1.2 mm, and 1 mm of rainfall accumulated over the four days between January 12 and 15. At site A5, a sharp decrease in radon concentration was observed on January 13, the day of significant rainfall, as shown in Fig. 6(a). The
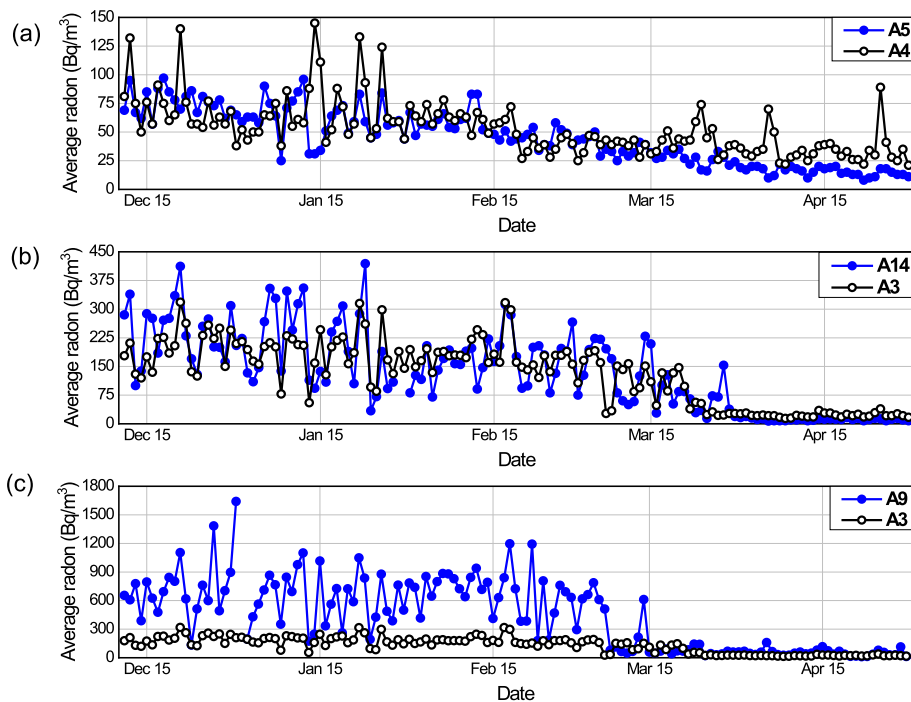

Fig. 5. Sites were grouped into 3 mutual distance ranges: (a) Group 1 as short distance, (b) Group 2 as middle distance, and (c) Group 3 as long distance—a selected day-average radon behavior in three groups.

Table 3

Distance groups (short, medium, and long) between two WCC facilities and their relative standard deviation (RSD).

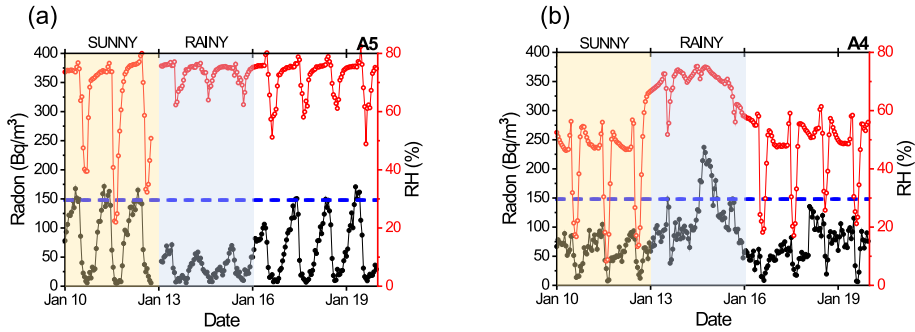| Group	WCC Facilities	Mutual Distance	RSD
Short distance	A4 & A5	1.82 km	0.1720
	A2 & A3	3.61 km	0.1681
Medium distance	A4 & A6	15.49 km	0.2522
	A3 & A14	16.3 km	0.3109
Long distance	A3 & A9	29.11 km	0.4991
	A3 & A8	29.89 km	0.6488

Fig. 6. Detailed view of radon concentration and RH from January 10 to 19 in sites of (a) A5 and (b) A4. Radon concentrations decreased in A5 but increased in A4 upon rain on January 13. The dashed lines are the recommended national standards.

radon concentration decreases as rain soaks into the ground and dilutes groundwater [25,26]. On January 14, the radon concentration reached its lowest point and slowly increased, returning to its usual level by January 17. The delayed maximum dilution may have been due to the slow infiltration of rainwater.

At site A4, which is located 1.8 km away from A5, the radon concentration in Fig. 6(b) did not decrease even on the day of rainfall. Instead, it started to increase from January 13, peaked on the January 14, and then decreased again to return to its usual level [27]. These phenomena could result from greater groundwater inflow from areas with higher radon concentrations than the surface rainwater inflow in area A4. This could be attributed to the difference in altitude of 9 m between A4 and A5, which is 119 and 128 m above sea level, respectively [28].

These results show that dilution caused by rainfall could occur only in high-altitude areas, whereas in low-altitude areas, complex compensatory phenomena involving the dilution and redistribution of groundwater could occur, resulting in abnormal radon concentrations on rainy days [29]. Rain-induced radon level fluctuations in areas with frequent rainfall need to be monitored for fine-level radon estimation.

3.4. Daily maximum radon concentrations versus ambient temperature

As previously stated, the daily maximum radon concentration usually occurs between 08:00 and 10:00, which is critical because
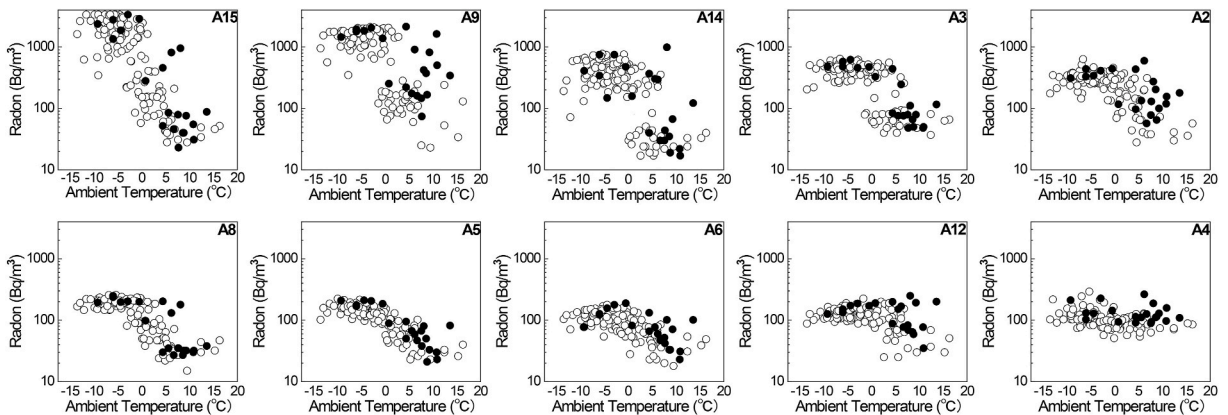

Fig. 7. Maximum radon concentration versus minimum ambient temperature on all days. Filled circles correspond to days with raindrops of 1 mm or more. Rearranged site order as descending maximum radon values.

workers begin their work early in the morning. As shown in the time-series plot in Fig. 3, relatively high radon concentrations were recorded during the winter season, whereas relatively low concentrations were recorded during the spring season at every site. Because the temperature inside the facilities was controlled during winter, we plotted the daily maximum radon concentration against the daily minimum ambient temperature obtained from the National Climate Data Center, as shown in Fig. 7. A single representative dataset for the ambient temperature was used because there was only one weather station in the study area. Five facilities with missing data (due to communication errors) were excluded, and the remaining ten sites were plotted and rearranged according to their maximum radon concentrations. We found that there were three distinctive regions of interest in the plots.

1. The minimum radon concentration region occurred when the outside temperature was higher than approximately 5 °C.
2. The maximum concentration region occurred when the temperature was less than 0 °C.
3. A transition region existed between the two temperature values.

Sites with a higher maximum radon concentration of approximately 1000 Bq/m^3 (A15, A9, A14, and A3) displayed the absence of the third transition region. In comparison, sites with lower maximum radon concentrations of approximately 200 Bq/m^3 (A2, A8, A5, A6, A12, and A4) exhibited a continuous transition region. The five excluded facilities showed similar behaviors; however, we excluded the integrity of the interpretation.

The WCCs with low radon concentrations (A12 and A4) had consistently low radon concentrations regardless of whether the water membrane was operational. The continuously increasing regions (A2–A6) exhibited low saturation levels with increasing groundwater usage. In contrast, areas with high radon concentrations (A15–A3) exhibited discrete behaviors, with high radon concentrations occurring only when the ambient temperature was low. As explained in Section 3.3, rainy days (filled circles) are located at the borders of the distribution, implying that rain-induced variations in groundwater cause abnormal radon release.

4. Discussion

In this study, the radon concentration in the soil was low. Even with groundwater usage, the radon concentration was relatively low before the water vapor condensation. The radon concentration increased rapidly at the water vapor saturation point, regardless of whether the radon source was soil or groundwater.

High radon concentrations in houses are due to radon's efficient diffusion or convection through ground surfaces [7]. In greenhouses, the exposure of the ground surface is greater than that in a typical house; therefore, it is reasonable to assume that the flow through the ground surface may be high. However, reported radon concentration measurements in greenhouses have shown diversities higher than or within the regulatory levels [8,30,31], indicating that more significant exposure to the ground surface does not imply a high radon risk. All the facilities in this study had radon concentrations within the regulatory range when the ambient temperature was above five °C, with significantly reduced groundwater usage. Therefore, a low-level baseline or continuous transitional increase in winter, as shown in Fig. 7, was caused by the release of radon from the soil and its accumulation in the facility. The slight increase in winter coincided with the higher radon content in buildings in winter than in spring, but the difference was only a few tens of percent [32,33]. The high radon concentrations with no transition regions shown in Fig. 7 are presumably due to the release of dissolved radon from groundwater sprayed into the air. If radon concentrations in groundwater are not high in some areas, there is no additional source, and only soil-originated radon accumulation is likely to occur in these areas. However, if the radon concentration in the groundwater is high, more radon is released into the air through spraying. Thus, WCC facilities are prone to a higher radon risk than ordinary greenhouses.

However, air-released radon did not accumulate in the facility until water vapor saturation, despite WCC operation. All the emitted radon quickly escaped into the atmosphere, resulting in significantly lower indoor radon concentrations before water vapor condensation. High radon concentrations in greenhouses occur only under high humidity conditions, even without water spraying [8, 31]. Radon has a strong ability to permeate microscopic pores [34]. We can imagine three different escape channels: pores in the soil, structural leakage paths in WCCs (such as overlapping polymer structures for ventilation), and direct transmission through the PE polymer, the primary material in the WCC facility. The permeation of radon through rock and soil pores is high but hampered by water vapor condensation [22]. The characteristic water vapor condensation on smooth surfaces and the highly selective permeability of radon can support direct transmission through PE polymers [34,35].

Although no single factor could play a role, radon successfully escaped from the WCC facility, resulting in insignificant radon values before water vapor saturation in our study. However, further studies on escaping channels are required to determine an effective radon mitigation method for WCCs. Natural ventilation through a channel depends on the structure or type of the WCCs [31,36]. Because we chose only one building structure to avoid structural dependency, the type of building structure dependency must be studied further to elucidate the escape of radon before water vapor condensation. The most straightforward mitigation option is simple ventilation; however, other options should be explored so plants are not exposed to low temperatures at dawn.

5. Conclusion

WCC facilities heated with groundwater during winter had radon concentrations above the national regulatory level. Radon levels varied significantly depending on the facility's operation, peaking when farmers began work in the early morning and then decreasing with ventilation. At all test sites, radon concentrations were insignificant without groundwater usage, suggesting that radon from the exposed soil was not a significant contributor. However, even during these low radon-level periods, relatively high values occurred at

night, when water vapor condensation occurred. During facility groundwater use, if water vapor condensation did not occur, radon came from the soil, and the groundwater escaped the facilities. When water vapor condensation occurs, radon accumulates rapidly depending on the degree of radon contamination in the groundwater. Groundwater contamination was evidenced by abnormal changes in radon concentrations due to regional rainfall and the accompanying dilution or inflow from other regions owing to groundwater movement. We concluded that groundwater contamination was the leading cause of high radon concentrations in the WCCs. But, without water vapor condensation in the facility, the radon emitted from the soil and groundwater escapes to the atmosphere through leakage paths, resulting in significantly lower indoor radon concentrations. Leakage paths and accumulation dynamics must be studied further. Our findings suggest potential avenues for mitigating radon in WCC facilities, including optimizing structural ventilation and controlling water vapor condensation.

Availability of data and materials

The datasets used and/or analyzed during the current study are available from the corresponding author upon reasonable request.

CRediT authorship contribution statement

Yelim Nam: Writing – original draft, Data curation. **Sangin Kim:** Investigation, Data curation. **Jihong Shin:** Software, Data curation. **Chaewon Yi:** Resources, Data curation. **Kyoung Sook Jeong:** Writing – review & editing, Validation, Formal analysis. **Seung Kyu Lee:** Writing – review & editing, Supervision. **Jiyoung Ko:** Visualization, Data curation. **Jongjin Lee:** Writing – review & editing, Validation, Supervision, Data curation, Conceptualization.

Declaration of competing interest

The authors declare that they have no known competing financial interests or personal relationships that could have appeared to influence the work reported in this paper.

Acknowledgments

Appendix A. Supplementary data

Supplementary data to this article can be found online at https://doi.org/10.1016/j.heliyon.2024.e30563.

References

[1] United Nations Scientific Committee on the Effects of Atomic Radiation, UNSCEAR 2000 Report, Volume I: Sources, United Nations, 2000.
[2] M. Al Jassim, R. Isaifan, A review on the sources and impacts of radon indoor air pollution, J Environ Toxicol Stud 2 (1) (2018).
[3] Radon and Health, WHO(World Health Organization), January 25, 2023. Available from: https://www.who.int/news-room/fact-sheets/detail/radon-and-health. (Accessed 8 June 2023).
[4] Health risk of radon. EPA(US Environmental Protection Agency), n.d., Available from: https://www.epa.gov/radon/health-risk-radon, accessed June 8, 2023.
[5] Indoor Air Quality Management Act. KLRI(Korea Legislation Research Institute), Available from: https://elaw.klri.re.kr/eng_service/lawView.do?hseq=41231&lang=ENG, accessed June 8, 2023.
[6] M.J. Focazio, D. Tipton, S. Dunkle Shapiro, L.H. Geiger, The chemical quality of self-supplied domestic well water in the United States, Groundwater Monitoring & Remediation 26 (3) (2006) 92–104.
[7] R.G. Sextro, Understanding the origin of radon indoors—building a predictive capability, Atmos. Environ. 21 (2) (1987) 431–438, 1967.
[8] X. Li, X. Xu, W. Li, F. Wang, C. Hai, Preliminary study on the variation of radon-222 inside greenhouse of Shouguang county, China, J. Environ. Radioact. 153 (2016) 120–125.
[9] K. Radon, B. Danuser, M. Iversen, E. Monso, C. Weber, J. Hartung, D. Nowak, Air contaminants in different European farming environments, Ann. Agric. Environ. Med. 9 (1) (2002).
[10] D.H. Jeong, M.S. Kim, B.K. Ju, T.S. Kim, Distribution characteristics of uranium and radon concentration in groundwaters of provinces in Korea, Journal of Soil and Groundwater Environment 16 (6) (2011) 143–149.
[11] D.S. Vinson, T.R. Campbell, A. Vengosh, Radon transfer from groundwater used in showers to indoor air, Appl. Geochem. 23 (9) (2008) 2676–2685.
[12] S.C. Kim, C.J. Park, J.H. Choi, M.A. Seo, J.G. Eom, M.S. Park, A study on the characteristics of indoor radon concentration in water curtain cultivation facilities, Journal of Environmental Analysis, Health and Toxicology 24 (2) (2021) 84–90.
[13] Y.S. Song, K.H. Park, Jiri Mountain, Korea: a window into the deep crust, The Journal of the Petrological Society of Korea 26 (4) (2017) 385–398.
[14] J. Seo, G. Kim, Rapid and precise measurements of radon in water using a pulsed ionization chamber, Limnol Oceanogr. Methods 19 (4) (2021) 245–252.
[15] C. Li, S. Zhao, C. Zhang, M. Li, J. Guo, N.T. Dimova, T. Yang, W. Liu, G. Chen, H. Yu, B. Xu, Further refinements of a continuous radon monitor for surface ocean water measurements, Front. Mar. Sci. 9 (2022) 1–10.
[16] W. Liu, C. Li, P. Cai, S. Zhao, J. Guo, W.C. Burnett, S. Song, G. Chen, B. Xu, Quantifying 224Ra/228Th disequilibrium in sediments via a pulsed ionization chamber (PIC), Mar. Chem. 245 (2022) 104160.
[17] W. Kada, N. Dwaikat, J. Datemichi, F. Sato, I. Murata, Y. Kato, T. Iida, A twin-type airflow pulse ionization chamber for continuous alpha-radioactivity monitoring in atmosphere, Radiat. Meas. 45 (9) (2010) 1044–1048.

[18] "Indoor air sampling and evaluation method" Korean law information center, Available at: https://www.law.go.kr/DRF/lawService.do?OC=me_pr&target=admrul&ID=2100000217816&type=HTML&mobileYn=. (Accessed 8 June 2023).

[19] National Climate Data Center of the Korea Meteorological Administration, Available at: https://data.kma.go.kr/resources/html/en/aowdp.html, accessed June 8, 2023.

[20] N.D. Chen, N.F. Chen, J. Li, C.Y. Cao, J.M. Wang, H.P. Huang, Similarity evaluation of different origins and species of Dendrobiums by GC-MS and FTIR analysis of polysaccharides, International Journal of Analytical Chemistry 2015 (2015) 8.

[21] V. Lednev, S.M. Pershin, A.F. Bunkin, Laser beam profile influence on LIBS analytical capabilities: single vs. multimode beam, J. Anal. Atomic Spectrom. 25 (11) (2010) 1745–1757.

[22] A. Fernandez-Cortes, D. Benavente, S. Cuezva, J.C. Cañaveras, M. Álvarez-Gallego, E. Garcia-Anton, S. Sanchez-Moral, Effect of water vapour condensation on the radon content in subsurface air in a hypogeal inactive-volcanic environment in Galdar cave, Spain, Atmos. Environ. 75 (2013) 15–23.

[23] G. Prasad, T. Ishikawa, M. Hosoda, A. Sorimachi, M. Janik, S.K. Sahoo, S. Uchida, Estimation of radon diffusion coefficients in soil using an updated experimental system, Rev. Sci. Instrum. 83 (9) (2012).

[24] K. Skeppström, B. Olofsson, A prediction method for radon in groundwater using GIS and multivariate statistics, Sci. Total Environ. 367 (2–3) (2006) 666–680.

[25] E. Hoehn, H.R. Von Gunten, Radon in groundwater: a tool to assess infiltration from surface waters to aquifers, Water Resour. Res. 25 (8) (1989) 1795–1803.

[26] S. Maeng, S.Y. Han, S.H. Lee, Analysis of radon depth profile in soil air after a rainfall by using diffusion model, Nucl. Eng. Technol. 51 (8) (2019) 2013–2017.

[27] S. De Francesco, F.P. Tommasone, E. Cuoco, G. Verrengia, D. Tedesco, Radon hazard in shallow groundwaters: amplification and long term variability induced by rainfall, Sci. Total Environ. 408 (4) (2010) 779–789.

[28] N.J. Mullinger, J.M. Pates, A.M. Binley, N.P. Crook, Controls on the spatial and temporal variability of 222Rn in riparian groundwater in a lowland Chalk catchment, J. Hydrol. 376 (1–2) (2009) 58–69.

[29] M. Fukui, 222Rn concentrations and variations in unconfined groundwater, J. Hydrol. 79 (1–2) (1985) 83–94.

[30] J.C. Santamarta, J. Rodríguez-Martín, N. Cruz-Pérez, Radon levels in greenhouses: a case study in Tenerife (Canary Islands), Int. J. Environ. Sci. Technol. 19 (4) (2022) 2877–2884.

[31] M. Abd El-Zaher, Radiation health hazard and risks assessment among greenhouse farmers in Egypt, seasonal study, Int. J. Radiat. Biol. 98 (8) (2022) 1388–1396.

[32] R.C. Ramola, M.S. Kandari, R.B.S. Rawat, T.V. Ramachandran, V.M. Choubey, A study of seasonal variations of radon levels in different types of houses, J. Environ. Radioact. 39 (1) (1998) 1–7.

[33] K.R. Kellenbenz, K.M. Shakya, Spatial and temporal variations in indoor radon concentrations in Pennsylvania, USA from 1988 to 2018, J. Environ. Radioact. 233 (2021) 106594.

[34] M. Jiránek, M. Kotrbatá, Radon diffusion coefficients in 360 waterproof materials of different chemical composition, Radiat. Protect. Dosim. 145 (2–3) (2011) 178–183.

[35] L. Tommasino, Passive sampling and monitoring of radon and other gases, Radiat. Protect. Dosim. 78 (1) (1998) 55–58.

[36] R. Yang, X. Zhang, X. Ye, C. Wang, X. Li, Ventilation modes and greenhouse structures affect 222 Rn concentration in greenhouses in China, J. Radioanal. Nucl. Chem. 323 (2020) 1103–1111.